Eur. Phys. J. C (2022) 82:896
https://doi.org/10.1140/epjc/s10052-022-10866-0

THE EUROPEAN PHYSICAL JOURNAL C

Regular Article - Theoretical Physics

Galaxy distributions as fractal systems

Sharon Teles[1,a], **Amanda R. Lopes**[2,3,b], **Marcelo B. Ribeiro**[4,c]

[1] Valongo Observatory, Universidade Federal do Rio de Janeiro, Rio de Janeiro, Brazil
[2] Department of Astronomy, Observatório Nacional, Rio de Janeiro, Brazil
[3] Instituto de Astrofísica de La Plata, CONICET-UNLP, La Plata, Argentina
[4] Physics Institute, Universidade Federal do Rio de Janeiro, Rio de Janeiro, Brazil

Received: 6 May 2022 / Accepted: 28 September 2022 / Published online: 10 October 2022

Abstract This paper discusses if large scale galaxy distribution samples containing almost one million objects can be characterized as fractal systems. The analysis performed by Teles et al. (Phys Lett B 813:136034, 2021) on the Ultra-VISTA DR1 survey is extended here to the SPLASH and COSMOS2015 catalogs, hence adding 750k new galaxies with measured redshifts to the studied samples. The standard ΛCDM cosmology having $H_0 = (70 \pm 5)$ km/s/Mpc and number density tools required for describing these galaxy distributions as single fractal systems with dimension D are adopted. We use the luminosity distance d_L, redshift distance d_z and galaxy area distance (transverse comoving distance) d_G as relativistic distance definitions to derive galaxy number densities in the redshift interval $0.1 \leq z \leq 4$ at volume limited subsamples defined by absolute magnitudes in the K-band. Similar to the findings of Teles et al. (2021), the results show two consecutive redshift scales where galaxy distribution data behave as single fractal structures. For $z < 1$ we found $D = 1.00 \pm 0.12$ for the SPLASH galaxies, and $D = 1,39 \pm 0.19$ for the COSMOS2015. For $1 \leq z \leq 4$ we respectively found $D = 0.83^{+0.36}_{-0.37}$ and $D = 0.54^{+0.27}_{-0.26}$. These results were verified to be robust under the assumed Hubble constant uncertainty. Calculations considering blue and red galaxies subsamples in both surveys showed that the fractal dimensions of blue galaxies as basically unchanged, but the ones for the red galaxies changed mostly to smaller values, meaning that D may be seen as a more intrinsic property of the distribution of objects in the Universe, therefore allowing for the fractal dimension to be used as a tool to study different populations of galaxies. All results confirm the decades old theoretical prediction of a decrease in the fractal dimension for $z > 1$.

[a] e-mail: steles.ts@gmail.com
[b] e-mail: amandalopes1920@gmail.com
[c] e-mail: mbr@if.ufrj.br (corresponding author)

1 Introduction

Fractal analysis of the galaxy distribution consists of applying the standard techniques of fractal geometry to a given galaxy redshift survey dataset with the aim of determining if this distribution has fractal features. In other words, the goal is to test the *fractal galaxy distribution hypothesis*, that is, the assumption that this distribution can be described as a fractal system. This analysis is done by calculating the key feature of fractal systems, the *fractal dimension* D, which basically characterizes the distribution's irregularity [46]. In the context of large-scale galactic clustering D basically determines galactic clustering sparsity or, complementarily, the dominance of voids in the distribution. If D is smaller than 3, which is the topological dimension where the fractal structure is embedded, it means that the structure has irregular patterns. Decreasing values of D means increasing sparsity in the galactic clustering [12,53,64].

The simplest way to characterize a fractal system is by means of the *single fractal dimension*, since it reduces the quantification of the irregular patterns within the system by means of a unique value for D. More complex structures can also be described by the single fractal approach, because a fractal system may possess different single values for D at different distance ranges, that is, single fractal systems in sequence at different data ranges [72]. The alternative way is called *multifractal*, where the fractal system has several fractal dimensions in the same scaling range, that is, a spectrum of dimensions whose maximum value corresponds to the single fractal dimension the structure would have if it were treated as a single fractal [23].

Galaxy redshift surveys datasets allow the determination of D by means of plots of observed number density vs. distance drawn from volume-limited samples. However, galaxies located at redshift depths where $z \gtrsim 0.1 - 0.2$ cannot

provide consistent volume densities without considering relativistic effects. That happens because relativistic cosmological models possess several distance definitions [20,21,33] and at those redshift ranges a single empirically determined value for z corresponds to different distance values. Moreover, in relativistic cosmology the geometrical locus of astronomical observations lies along the past light cone, which means that even spatially homogeneous cosmological models like the standard Friedmann–Lemaître–Robertson–Walker (FLRW) are characterized by observational inhomogeneities at high redshift ranges [55], since any distance measure required in the determination of volume densities will necessarily depart the local spatially homogeneous hypersurfaces of these models at $z \gtrsim 0.1 - 0.2$ [57,60]. Hence, relativistic effects need to be taken into account when fractal analyses are performed from moderate to high redshift ranges [62].

The discussion above summarizes the scope of *fractal cosmology*, as consisting of modeling the large-scale structure of the Universe by assuming that its galaxy distribution behaves as a fractal pattern. It has been previously known in the literature as *hierarchical cosmology* due to discussions regarding the possible hierarchical structuring of the Universe in the beginning of the 20th century [5,10,11,19,68]; see also [32], pp. 410–412, 1975–1976. Attempts to theoretically describe and empirically characterize this hierarchical galaxy structure were also proposed [8,16,17,31,74,75] (see also [32], pp. 371–372, 572–574), nevertheless, after the appearance of fractal geometry in the 1980s it became clear that the old hierarchical cosmology concepts are essentially the same as those of fractal cosmology, leading in fact to the same expressions, albeit with different terminology [59,64].

Early hierarchical cosmology models were proposed within the framework of Newtonian cosmology [31,74,75], as well as in more recent fractal cosmology ones [1,2]. Later on relativistic fractal cosmologies considering a fractal system embedded in a 4-dimensional spacetime along the observer's past light cone were proposed [3,56,58,61–63]. Other authors have also discussed relativistic cosmological models with theoretical fractal features [7,14,36,42,49–51,65,71,76] or by assuming single fractal or multifractal patterns in observational scenarios using Newtonian or relativistic models [24–27,43,47,52,54,69,70].

The question of whether or not there would be a transition to homogeneity in the galaxy distribution at some yet to be determined scale is still observationally controversial. Some recent studies argue that the latest galaxy distribution data indicate a transition to homogeneity [28–30,67], whereas others disagree with such a conclusion [9,13,15,73]. This observational tension seems to be a result of sometimes using shallow galaxy redshift data, and how data is theoretically interpreted and statistically handled, not infrequently due to the unwarranted assumption that relativistic effects can be ignored in fractal cosmology studies [55,62,63]. We shall return to this point below.

In addition, it must be mentioned the now decades old theoretical prediction that a possible galaxy fractal structure must lead to a decrease in the fractal dimension for $z > 1$ even in spatially homogeneous FLRW cosmologies. This is due to the fact that in these cosmologies the volume density significantly decreases at such scales when calculated along the past light cone, as it must be, and that inevitably leads to a decrease in the fractal dimension D beyond that range see: [57], Fig. 1; [60], Figs. 1 and 3; [62], Fig. 2.

Another source for this observational tension lies on the difficulties for testing the fractal galaxy distribution hypothesis at large-scales due to, until recently, lack of data at $z > 2$, or insufficient galaxy numbers with measured redshifts at $1 < z < 2$. Nevertheless, Conde-Saavedra et al. [13] were able to test this hypothesis using the FORS Deep Field (FDF) dataset consisting of 5558 galaxies in the range $0.45 \leq z \leq 5.0$, and concluded that at $z \lesssim 1.3 - 1.9$ the sample presented an average single fractal dimension of $D = 1.4^{+0.7}_{-0.6}$, whereas beyond this threshold they obtained $D = 0.5^{+1.2}_{-0.4}$. This study provided the first observational support for the above mentioned theoretical prediction of a decreasing fractal dimension at larger scales, even despite the relatively high data uncertainties in the measure of D ensued by the indirect luminosity function method employed by the authors to obtain volume-limited samples.

This line of investigation was further advanced by [73], who carried out a fractal analysis of the UltraVISTA DR1 survey containing 219,300 measured redshift galaxies, a sample considerably larger than the FDF one, and obtained volume-limited samples directly from measured redshift data instead of the indirect luminosity function methodology. This study was performed considering a FLRW cosmological model, and led to improved results in terms of better defined threshold for moderate and high scaling ranges, smaller uncertainties and results more in line with each other considering all cosmological distance definitions. They reached at conclusions similar to [13], i.e., that a volume-limited subsample of the UltraVISTA DR1 galaxy distribution can also be characterized as a fractal system with two consecutive scaling ranges with the following median dimensions and uncertainties: $D = (1.58 \pm 0.20)$ for $z < 1$, and $D = (0.59 \pm 0.28)$ for $1 \leq z \leq 4$. These results provided further empirical support to the early theoretical prediction of a decrease in the fractal dimension at larger scales.

This work aims at extending the study carried out by Teles et al. [73] in addition to testing if the fractal dimension changes for different galaxy type subsamples. It applies the same methodology and underlying cosmology, but uses instead data from the COSMOS2015 and SPLASH redshift surveys. The former galaxy catalog considerably enlarged the UltraVISTA DR1 number of galaxies observed in the same

northern hemisphere observational field, almost tripling the total number of objects, from 219,300 to 578,379, whereas the latter has 390,362 objects with measured redshifts surveyed in a portion of the southern hemisphere. Together they added almost 750k new galaxies up the $z = 6$ in comparison to the number of objects studied by [73], providing then a considerably larger galaxy distribution sample to perform fractal analysis.

The conclusions reached here provide further empirical support that the galaxy distribution can be characterized by two subsequent fractal scaling ranges at decreasing single fractal dimension values and with no detectable transition to homogeneity up to the redshift limits of both surveys. Two volume-limited subsamples were generated in both surveys by means of filtering through absolute magnitudes obtained in the K-band. For $z < 1$ we obtained $D = 1.00 \pm 0.12$ for the SPLASH galaxies, and $D = 1,39 \pm 0.19$ for the COSMOS2015. For $1 \leq z \leq 4$ we respectively found $D = 0.83^{+0.36}_{-0.37}$ and $D = 0.54^{+0.27}_{-0.26}$. These results turned out to be robust under the adopted Hubble constant uncertainty of $H_0 = (70 \pm 5)$ km/s/Mpc.

Further subsamples were generated by selecting blue, star forming, galaxies and red, quiescent, ones and subsequently filtering them through the same absolute magnitude criterion described above. The fractal dimensions of blue galaxies turned out either unchanged or only marginally changed as compared to the unselected and filtered samples. However, the red galaxies had their fractal dimensions becoming noticeably smaller in most cases, apart from the red COSMOS1015 whose D values increased, also noticeably.

Such results suggest that single fractal dimensions may be used not only as a descriptors of galaxy distributions, but also as tools to trace galaxy types and/or their evolutionary stages at different redshift ranges. Besides, all results obtained here provide further empirical confirmation of the theoretical prediction of a decrease in the fractal dimensions at ranges where $z > 1$.

The plan of the paper is as follows. Section 2 summarizes the essential tools of relativistic fractal geometry required for testing the fractal galaxy distribution hypothesis. Section 3 describes the observational details of the COSMOS2015 and SPLASH redshift surveys relevant to this work, as well as the data handling required for the application of fractal tools to these datasets. Section 4 presents the results of the fractal analysis of the COSMOS2015 and SPLASH galaxy distributions, comparing them with previous results reached with the UltraVISTA DR1 and FDF surveys. Section 5 presents fractal dimensions by generating blue, star forming, and red, quiescent, galaxy subsamples of the COSMOS2015 and SPLASH datasets, and compares the results with the ones obtained with their respective unselected samples showed in the previous section. Section 6 presents our conclusions.

2 Relativistic fractal cosmology

Fractal systems are characterized by power-laws, property known since Mandelbrot's [46] original studies on fractals. Indeed, the connection of early galactic structure observations to hierarchical cosmology, and then to fractals, was done through the *observed* power-law features of galaxy distribution [17,53]. Naturally, the relativistic fractal cosmology definitions and concepts can only make sense if conceived in this same context, that is, power-law relationships among *observable quantities*. This section presents a brief review of concepts and definitions appropriate for the description of possible fractal patterns in the galaxy distributions at moderate and large redshift scales [see 73, Sec. 2,formoredetails].

Let $V_{\rm obs}$ be the *observational volume* defined as follows,

$$V_{\rm obs} = \frac{4}{3}\pi\,(d_{\rm obs})^3, \tag{1}$$

where $d_{\rm obs}$ is an *observational distance*. The *observed number density* $\gamma^*_{\rm obs}$ is given by,

$$\gamma^*_{\rm obs} = \frac{N_{\rm obs}}{V_{\rm obs}}, \tag{2}$$

where $N_{\rm obs}$ is the *observed cumulative number counts* of cosmological sources, that is, galaxies. It is clear that $\gamma^*_{\rm obs}$ gives the number of sources per unit of observational volume out to a distance $d_{\rm obs}$, in addition to being a radial quantity and, thus, cannot be understood in statistical sense because it does not average all points against all points.

The *Pietronero–Wertz hierarchical (fractal) cosmology model* [59], Sec. 3; [64], Sec. III.4 has as key underlying hypothesis a phenomenological expression called the *number-distance relation*, written as follows,

$$N_{\rm obs} = B\,(d_{\rm obs})^D, \tag{3}$$

where B is a positive constant and D is the single fractal dimension. If in the expression above $D = 3$, $N_{\rm obs}$ grows with $V_{\rm obs}$ and galaxies would evenly distribute along all regions of the observed space. However, if $D < 3$, as $d_{\rm obs}$ increases $N_{\rm obs}$ grows at a smaller pace than $V_{\rm obs}$, creating then gaps in the galactic distribution, that is, regions devoid of galaxies. Alongside these galactic gaps there would be regions where galaxies clump. Therefore, voids and galactic clumpiness would be a by-product of a fractal galaxy structure whose fractal dimension is smaller than the topological dimension where the galaxy structure is embedded. In this scenario the fractal dimension becomes a descriptor of galactic clumpiness or, complementarily, the dominance of voids in the galactic structure.

One must note that $N_{\rm obs}$ is a cumulative quantity. So, if beyond a certain distance there are no longer galaxies then $N_{\rm obs}$ no longer increases with $d_{\rm obs}$. If, on the other hand, objects are still detected and counted, even at irregular pace,

then it continues to increase. This rate of growth can be affected by observational biases, possibly leading to an intermittent behavior, however $N_{\rm obs}$ must grow or remain constant and, therefore, the exponent in Eq. (3) must be positive or zero.

Substituting Eqs. (1) and (3) into Eq. (2) we obtain the *De Vaucouleurs density power-law* [53,59],

$$\gamma^*_{\rm obs} = \frac{3B}{4\pi}(d_{\rm obs})^{D-3}. \tag{4}$$

Hence, if the observed galaxy distribution is found to have $D < 3$, the observational number density above decays as a power-law. If $D = 3$ galaxies are evenly distributed and the galactic structure is said to be *observationally homogeneous*. In this case the number density becomes constant and distance independent. Smaller values of D imply steeper power-law decays and, consequently, more gaps in the galaxy distribution. Note that the power-law above allows for the empirical determination of different fractal dimensions in two or more scaling ranges dependent on the intervals of $d_{\rm obs}$.

The expressions above are directly applicable in Newtonian cosmology, however, to use them in a relativistic setting some relativistic concepts must come to the forefront. First, in relativistic cosmology the geometrical locus of observations is the observer's past light cone, which means that that even spatially homogeneous cosmologies like the FLRW will *not* produce observationally constant number densities at moderate or high redshift values because this is theoretically prohibited [13, Sec. 2.1]. As discussed at length elsewhere [55], observational and spatial homogeneities are different relativistic concepts in cosmology, thus, even a cosmological-principle-obeying spatially homogeneous cosmological model will exhibit observational inhomogeneities at moderate and high redshift ranges [see also 57,59,60,62,63]. Therefore, $\gamma^*_{\rm obs}$ is an average relativistic density and *must not be confused with* the fluid approximation local density ρ appearing on the right hand side of the Einstein equations.

Second, theoretical calculations of $\gamma^*_{\rm obs}$ along the past light cone in the FLRW cosmologies had already predicted that a decay of $\gamma^*_{\rm obs}$ at increasing observation distances is to be observationally expected [57], Fig. 1; [60], Figs. 1, 3; [62], Fig. 2, which means that dealing with observations even in FLRW, or FLRW like, cosmology backgrounds should lead to a decrease for D at $z > 1$.

The third important relativistic concept that one must bear in mind when dealing with relativistic fractal cosmologies is that number densities in fractal cosmology are defined in terms of observational distances, which means that at high redshift $d_{\rm obs}$ will have different values for each distance definition at the same redshift value z. This means that as distance in relativistic cosmology is not uniquely defined [20,21,33–35] $d_{\rm obs}$ must be replaced by d_i in the equations above. The index indicates the observed distance measure chosen to be calculated with a specific redshift value. The distance definitions applicable to relativistic fractal cosmology are the *luminosity distance* d_L, *redshift distance* d_z, and *galaxy area distance* d_G, also known as *transverse comoving distance*. Two of these distance definitions are connected by the Etherington reciprocity law below [21,22],

$$d_L = (1+z)\, d_G. \tag{5}$$

The redshift distance is defined as,

$$d_z = \frac{c\, z}{H_0}, \tag{6}$$

where c is the light speed and H_0 is the Hubble constant.

Fractal analyses can be performed using d_L and d_G in any cosmological model, however Eq. (6) is only valid in FLRW cosmologies. Besides, some caution is necessary with d_G because its respective volume density in the Einstein-de Sitter cosmology results in γ^*_G = constant [62, pp. 1718, 1723-1724], although this is not true in all FLRW models, because Albani et al. [4, Fig. 7] and Iribarrem et al. [41, Figs. 1-12] showed that in the ΛCDM cosmology the number densities obtained with these three relativistic distances possess decaying power-law properties. This conclusion justifies their adoption in the present study. In addition, although D can be calculated with any distance, the comoving distance could be seen as more appropriate because this is the distance where one often assumes homogeneity to be present when one projects galaxies and fluctuations in cosmology.

Bearing these points in mind, the expressions above must be rewritten as below in order to become applicable to relativistic cosmologies:

$$d_{\rm obs} = d_i, \tag{7}$$

$$V_{\rm obs} = V_i = \frac{4}{3}\pi (d_i)^3, \tag{8}$$

$$N_{\rm obs} = N_i = B_i\, (d_i)^{D_i}, \tag{9}$$

$$\gamma^*_{\rm obs} = \gamma^*_i = \frac{N_i}{V_i} = \frac{3B_i}{4\pi}(d_i)^{D_i-3}, \tag{10}$$

where $i = (L,\ z,\ G)$ according to the chosen distance definition. The constant B_i becomes attached to each specific distance, the same being true for the fractal dimension D_i. This is so because N_i is counted considering the limits given by each distance definition, which means that for a given z each d_i will produce its respective V_i, N_i, B_i and D_i. Hence, all quantities become attached to a certain distance definition

As final comments, one must stress again the difference between spatial and observation number densities, difference which arises only when the relativistic concept of past light cone, the geometrical locus of astronomical observations, is taken into account when modeling fractal cosmology at moderate and high redshift scales. So, only by correctly manipulating the theoretical tools of relativistic cosmological models

that the possible large-scale fractality of galaxy distribution will be revealed [55,60,62,63].

3 Fractal analysis

Testing the fractal galaxy distribution hypothesis was done with galaxy datasets provided by the COSMOS2015 and SPLASH redshift surveys. Both catalogs contain hundreds of thousands additional galaxies with measured redshifts as compared to the UltraVISTA DR1 dataset studied by Teles et al. [73]. Details on these surveys relevant to the present study, followed by the fractal analyses performed in their respective datasets, are shown below.

3.1 The COSMOS2015 galaxy redshift survey

The COSMOS2015 catalog [44] includes YJHK$_S$ images from the UltraVISTA DR2, Y-band images from Subaru/Hyper-Suprime-Cam and infrared data from the Spitzer Large Area survey over 2 deg^2 in the COSMOS field [66]. The object detection is performed by the χ^2 sum of the YJHK$_S$ and z^{++} images. Based on these data the UltraVISTA DR2 region contains 578,379 galaxies, which means that 359,079 new objects were added to the sample as compared to the 219,300 galaxies comprising the UltraVISTA DR1. The observed area has the following range of coordinates: $1.61 \leq$ Dec (deg) ≤ 2.81 and $149.31 \leq$ Ra (deg) ≤ 150.79, in which the full region has a limiting magnitude $K_S = 24.0$ at 3σ in a 3" diameter aperture and parts of the field covered by the "ultra-deep stripes" (0.62 deg^2) have limiting magnitude $K_S = 24.7$ at 3σ in a 3" diameter. The photometric redshifts were computed using LePHARE [6,38] following [40]. The total sample has $0.1 \leq z \leq 6$, with a very sizable number of galaxies located in the scale of $1 < z < 4$ (see Fig. 1). Hence, these features placed the additional galaxies provided by this survey well within the purposes of this study.

3.2 The SPLASH galaxy redshift survey

The SPLASH survey is a deep field galaxy redshift catalog with multi-wavelength photometry within 2.4 deg^2 in the sky region of $-5.64 \leq$ Dec (deg) ≤ -4.35 and $33.84 \leq$ Ra (deg) ≤ 35.16 [48]. The sources were identified using a detection image defined as a χ^2 combination of grzy images from Hyper-Suprime-Cam (HSC) DR1, JHK images from Ultra Deep Survey (UDS) DR11, YJHK$_S$ images from VISTA Deep Extragalactic Observations (VIDEO), u image from Megacam Ultra-deep Survey: U-Band Imaging (MUSUBI), and ugri images from CFHT Legacy Survey (CFHTLS). This catalog contains 390362 galaxies at $0 < z < 6$, where the redshifts were measured using LePHARE with a similar approach to that used for the COSMOS field [40,44]. The galaxy number distribution in terms of the redshift is shown in Fig. 1, where it is clear that a sizable portion of its galaxies are in the redshift interval $1 < z < 4$, a fact that justifies its inclusion in this fractal analysis, Besides, the SPLASH galaxies were mapped in a different sky region as compared to the surveys discussed above, and it follows a different strategy for the detection of the objects, as it includes the u-band, in order to recover the bluest objects.

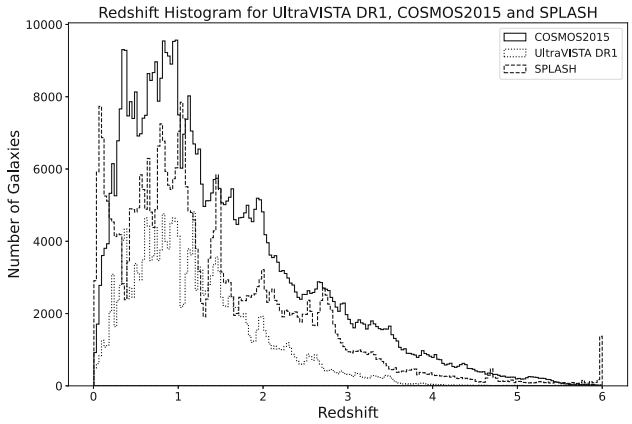

Fig. 1 Histogram showing the galaxy distribution numbers in terms of redshift for the SPLASH, UltraVISTA DR1 and COSMOS2015 surveys

3.3 Data filtering

Fractal analysis of galaxy surveys requires disposing the data along volume-limited distributions. As galaxy surveys are limited by apparent magnitude, we must proceed by reducing the data into subsamples such that they follow increasing redshift bins. This is done by plotting the absolute magnitudes of galaxies in terms of their respective measured redshifts, and then by only choosing galaxies below a certain absolute magnitude threshold defined by the limiting apparent magnitude of the survey. The usual expression

$$M = m - 5\log d_L(z) - 25, \tag{11}$$

where M is the absolute magnitude, m is the apparent magnitude and d_L is given in Mpc, can be used for this purpose. We assumed the FLRW cosmology with $\Omega_{m_0} = 0.3$, $\Omega_{\Lambda_0} = 0.7$ and $H_0 = (70 \pm 5)$ km s^{-1} Mpc^{-1}.

Next, the apparent magnitude threshold in the K-band was assumed to be $K = 24.7$, a mean limiting value acceptable to both surveys (see [73]) such that homogeneous volume-limited subsamples could be created by changing Eq. (11) to the expression below,

$$M_K = 24.7 - 5\log d_L(z) - 25, \tag{12}$$

which provides the cutoff line between the filtered and unfiltered galaxies. Finally, this whole process was made effective considering the above uncertainty in the Hubble constant

in order to test to what extent, if any, our results would be affected by its error margin.

Figure 2 shows the selection of the COSMOS2015 survey obtained according to the filtering procedure described above. Only galaxies with absolute magnitudes M_K above the cutoff line were included in a subsample for further analysis. In addition, we also disregarded galaxies having $z > 4$ as, according to Fig. 1, their numbers are too small to be considered representative. The end result of this process was the creation of three subsamples containing 230,705 galaxies in the redshift range $0.004 \leq z \leq 4$ out of the original 578,379 objects for three values of the Hubble constant within its uncertainty.

Figure 3 shows the same filtering procedure carried out with the SPLASH galaxies generating three other subsamples as well. The original 390362 objects were then reduced to 171548 galaxies.

3.4 Data analysis

The above parameters for the FLRW cosmology allowed the calculation of the observational distances d_i ($i = G, L, z$) using theoretical expressions relating distance to redshift provided by this cosmological model with the photometric redshift values furnished by the galaxy surveys. The data sorting algorithm necessary for carrying out a fractal analysis under the theoretical model discussed in Sect. 2 above is the same as employed by Teles et al. [73]. It is suscintly described as follows.

We started by establishing the minimum redshift value z_0, the respective minimum distances $d_{i_0} = d_{i_0}(z_0)$, and the incremental distance interval Δd_i. The algorithm was initiated by counting the number of observed galaxies N_{i_1} in the first interval $d_{i_1} = d_{i_0} + \Delta d_i$ and calculating the respective volume density $\gamma^*_{i_1}$. This defined the first bin. The next step was to increase the bin size by Δd_i. Values for N_{i_2} and $\gamma^*_{i_2}$ were then calculated at the distance $d_{i_2} = d_{i_0} + 2\Delta d_i$. These steps were repeated n times until the farthest group of galaxies were included and all quantities of interest counted and calculated.

We tested different bin size increments Δd_i for each distance definition to see if the results would be affected, with negative results. Therefore, the interval $\Delta d_i = 200$ Mpc was applied to all calculations, choice which in the end provided a large amount of data points for all quantities involved, allowing then enough points to perform adequate regression analyses.

Finally, according to Eq. (10) plots of γ^*_i vs. d_i would behave as decaying power-law curves if the galaxy distribution really formed a fractal system. In this case the linear fit slopes in log–log plots would allow for the fractal dimensions D_i of the distribution to be directly determined.

4 Results

Figures 4, 5, 6, 7, 8 and 9 show log–log graphs of γ^*_i vs. d_i with both surveys' datasets studied here with their respective choices of Hubble constant values within the above defined uncertainty. The results show that the galaxy distribution in both surveys present power-law decays in two scale ranges: for $z < 1$ and $1 \leq z \leq 4$. This is consistent with a fractal system possessing two single fractal dimensions at different distance ranges.

The fractal dimensions in both scaling ranges can be simply calculated from the slopes of the fitted straight lines by means of Eq. (10). All obtained results are collected in Tables 1, 2, 3 and 4, where one can clearly verify two single fractal systems in sequence at different data ranges with decreasing values for D at higher redshift ranges, as theoretically predicted (see Sect. 1 above). Besides, the results show the fractal dimensions being unaffected by variations in the Hubble constant.

One can summarize all results of Tables 1, 2, 3 and 4 by conservatively rounding off the main results and uncertainties around their medians. Hence, for $z < 1$ the COSMOS2015 survey produced $D = 1.4 \pm 0.2$, whereas the SPLASH galaxies yielded $D = 1.0 \pm 0.1$. For $1 \leq z \leq 4$ we respectively found $D = 0.5 \pm 0.3$ and $D = 0.8 \pm 0.4$. Clearly the SPLASH galaxies produce fractal dimensions somewhat smaller than the COSMOS2015 ones for $z < 1$, but the reverse situation for $z > 1$, although with overlapping uncertainties. Possible reasons for such differences and comparison with previous studies will be discussed below.

Finally, for comparison of fractal dimensions obtained with similar methodology as described here, Table 5 presents all values for D calculated with the UltraVISTA DR1, COSMO2015, SPLASH and FDF surveys when assuming $H_0 = 70$ km/s/Mpc.

5 Blue and red subsamples

All single fractal dimensions presented so far were calculated without any consideration of galactic types, features or possible evolutionary stages. Hence, one may wonder if D could depend on some, or all, of these characteristics, however they are defined or observed. If such possible dependencies are actually found, fractal dimensions could, perhaps, be used as tracers of galactic properties or their evolutionary stages. Below we propose a simple test of this possible dependency using the surveys studied here.

The COSMOS2015 and SPLASH data allow us to calculate D in two galaxy subsamples: the blue, or star forming, and the red, or quiescent, galaxies. Such a selection provides a preliminary and straightforward way of testing the con-

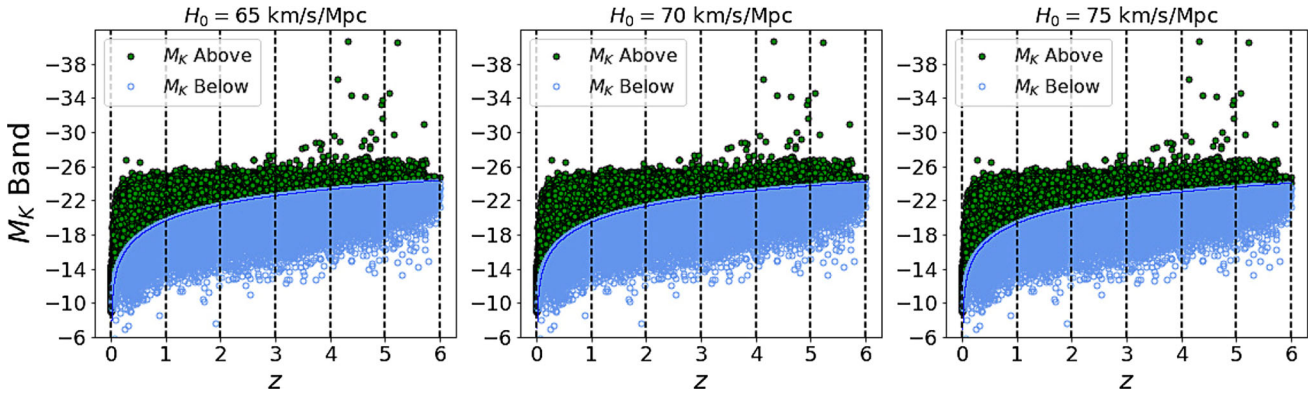

Fig. 2 Plot of the absolute magnitudes for the COSMOS2015 galaxies in terms of of their photometrically measured redshift values. The dividing line corresponds to apparent magnitude K = 24.7 and only galaxies having M_{K} above this cutoff and $z \leq 4$ were included in subsamples that assumed three different values of the Hubble constant

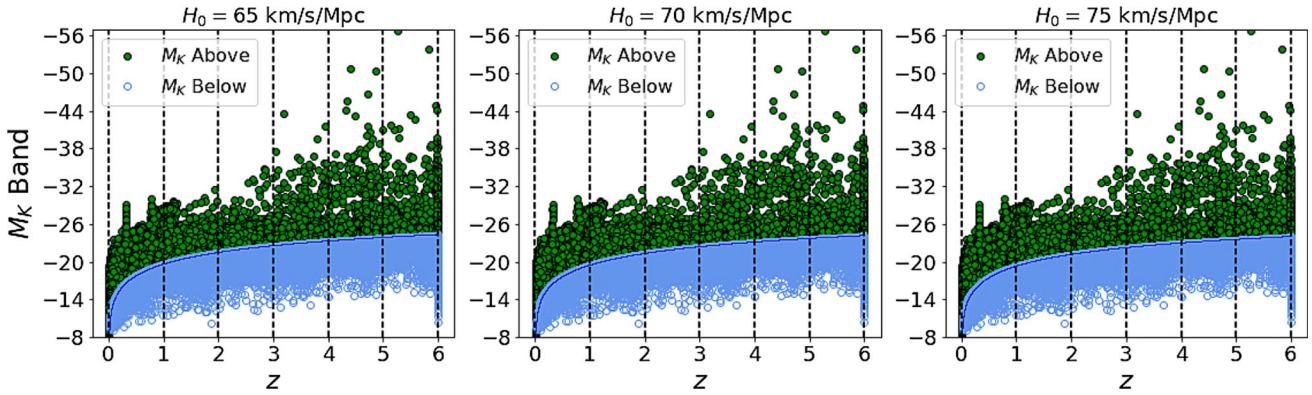

Fig. 3 Plot of the absolute magnitudes for the SPLASH galaxies in terms of of their photometrically measured redshift values. The dividing line corresponds to apparent magnitude K = 24.7 and only galaxies having M_{K} above this cutoff and $z \leq 4$ were included in subsamples that assumed three different values of the Hubble constant within its uncertainty

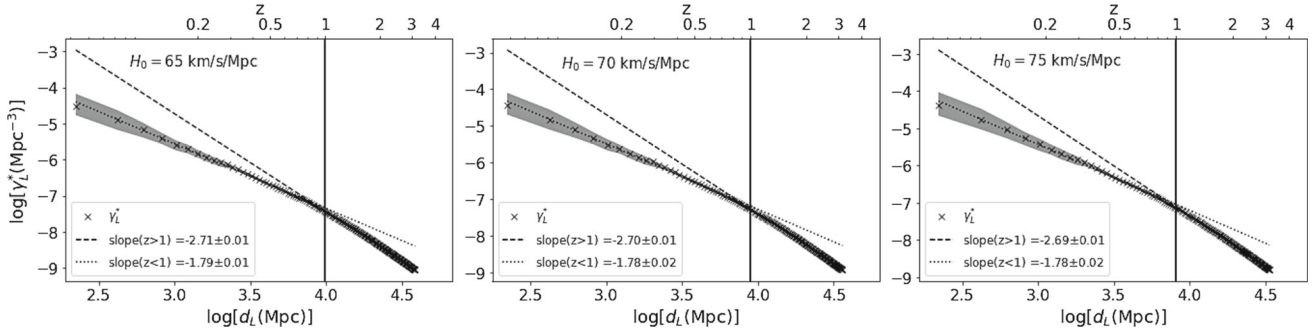

Fig. 4 Log–log graph of γ_L^* vs. d_L obtained with the COSMOS2015 galaxy redshift survey dataset in the ranges $z < 1$ and $1 \leq z \leq 4$ and respective distance measures

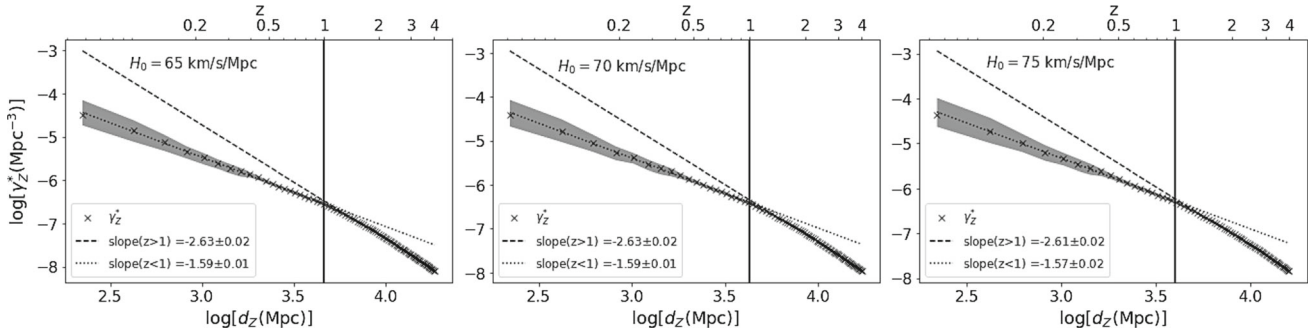

Fig. 5 Log–log graph of γ_z^* vs. d_z obtained with the COSMOS2015 galaxy redshift survey dataset in the ranges $z < 1$ and $1 \leq z \leq 4$ and respective distance measures

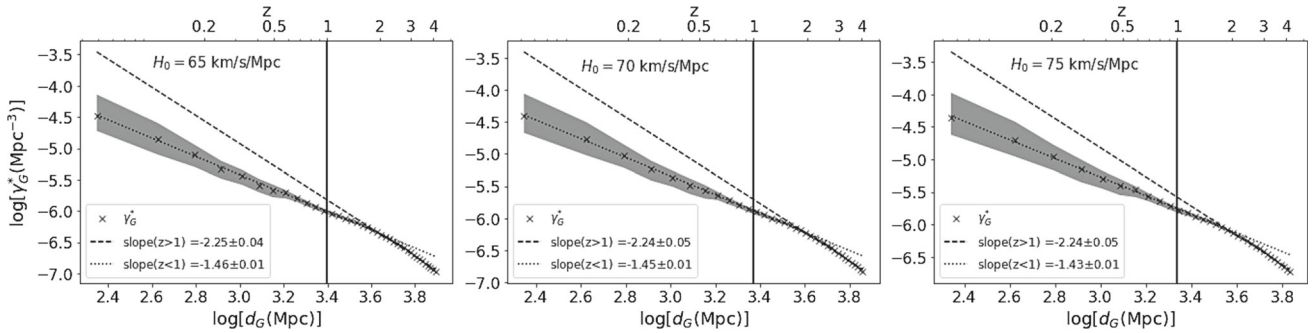

Fig. 6 Log–log graph of γ_G^* vs. d_G obtained with the COSMOS2015 galaxy redshift survey dataset in the ranges $z < 1$ and $1 \leq z \leq 4$ and respective distance measures

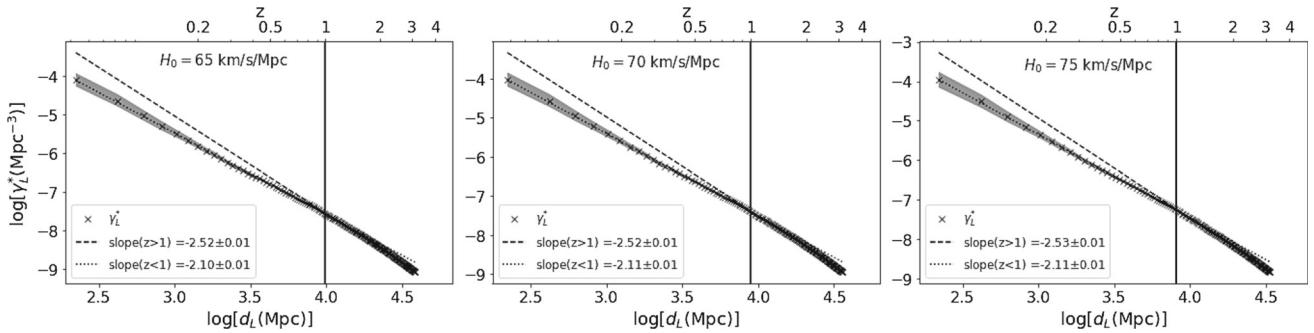

Fig. 7 Log–log graph of γ_L^* vs. d_L obtained with the SPLASH galaxy redshift survey dataset in the ranges $z < 1$ and $1 \leq z \leq 4$ and respective distance measures

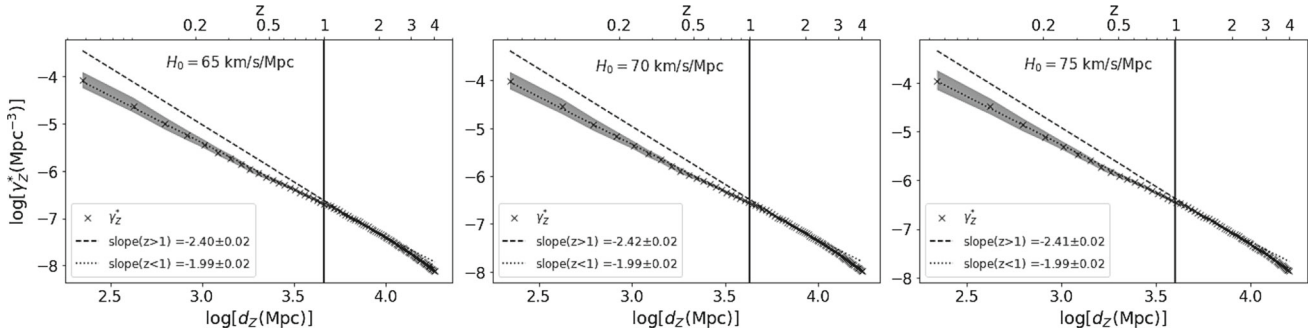

Fig. 8 Log–log graph of γ_z^* vs. d_z obtained with the SPLASH galaxy redshift survey dataset in the ranges $z < 1$ and $1 \leq z \leq 4$ and respective distance measures

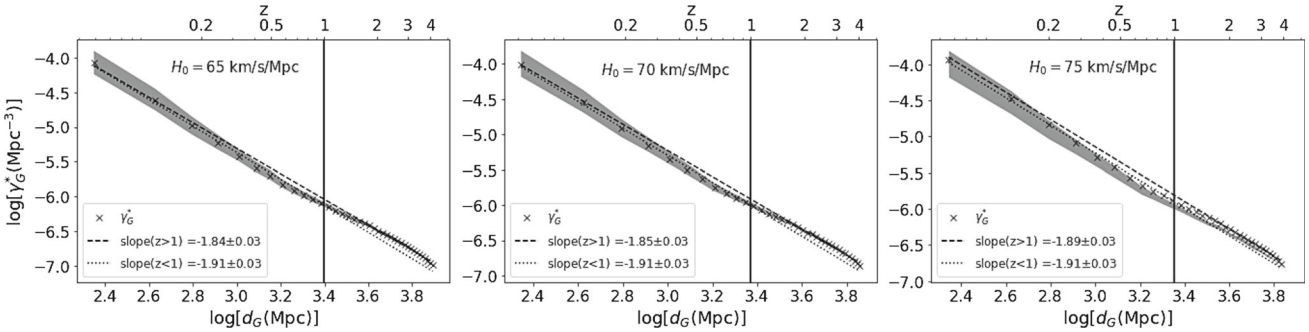

Fig. 9 Log–log graph of γ_G^* vs. d_G obtained with the SPLASH galaxy redshift survey dataset in the ranges $z < 1$ and $1 \leq z \leq 4$ and respective distance measures

Table 1 Fractal dimensions calculated in the reduced and volume-limited subsamples of the COSMOS2015 galaxy redshift survey in the range $z < 1$. The single fractal dimensions D_L, D_z and D_G were obtained from the galaxy distributions respectively using the luminosity distance d_L, redshift distance d_z and galaxy area distance (transverse comoving distance) d_G

$z < 1$	D_L	D_z	D_G
$H_0 = 65$ km/s/Mpc	1.21 ± 0.01	1.41 ± 0.01	1.54 ± 0.01
$H_0 = 70$ km/s/Mpc	1.22 ± 0.02	1.41 ± 0.01	1.55 ± 0.01
$H_0 = 75$ km/s/Mpc	1.22 ± 0.02	1.43 ± 0.02	1.57 ± 0.01

Table 2 Fractal dimensions obtained with the COSMOS2015 survey subsamples in the range $1 \leq z \leq 4$. Quantities are as described in Table 1

$1 \leq z \leq 4$	D_L	D_z	D_G
$H_0 = 65$ km/s/Mpc	0.29 ± 0.01	0.37 ± 0.02	0.75 ± 0.04
$H_0 = 70$ km/s/Mpc	0.30 ± 0.01	0.37 ± 0.02	0.76 ± 0.05
$H_0 = 75$ km/s/Mpc	0.31 ± 0.01	0.39 ± 0.02	0.76 ± 0.05

Table 3 Fractal dimensions obtained with the SPLASH survey subsamples in the range $z < 1$. Quantities are as described in Table 1

$z < 1$	D_L	D_z	D_G
$H_0 = 65$ km/s/Mpc	0.90 ± 0.01	1.01 ± 0.02	1.09 ± 0.03
$H_0 = 70$ km/s/Mpc	0.89 ± 0.01	1.01 ± 0.02	1.09 ± 0.03
$H_0 = 75$ km/s/Mpc	0.89 ± 0.01	1.01 ± 0.02	1.09 ± 0.03

Table 4 Fractal dimensions obtained with the SPLASH survey subsamples in the range $1 \leq z \leq 4$. Quantities are as described in Table 1

$1 \leq z \leq 4$	D_L	D_z	D_G
$H_0 = 65$ km/s/Mpc	0.48 ± 0.01	0.60 ± 0.02	1.16 ± 0.03
$H_0 = 70$ km/s/Mpc	0.48 ± 0.01	0.58 ± 0.02	1.15 ± 0.03
$H_0 = 75$ km/s/Mpc	0.47 ± 0.01	0.59 ± 0.02	1.11 ± 0.03

cept of possible use of D as a tracer of galactic features.[1] The criteria for generating these subsamples use color–color diagrams or star formation rates as provided in both surveys databases.

For the COSMOS2015 dataset, the classification presented in [44] is derived from the location of galaxies in the NUV-r vs. r-J color–color diagram [77]. Besides using these colors, this selection has the estimation of the absolute magnitudes at rest-frame based on the apparent magnitudes at $\lambda_{\text{rest-frame}}(1+z_{\text{gal}})$, which minimises the k-correction dependency [37]. Such technique avoids the mixing between red dusty galaxies and quiescent ones. In practice, included quiescent galaxies have $M_{\text{NUV}} - M_{\text{r}} > 3\,(M_{\text{r}} - M_{\text{J}}) + 1$

[1] We are grateful to a referee for suggesting this test.

Table 5 This table presents a comparison of all recently calculated single fractal dimensions applying similar analytical tools as presented here to various galaxy distribution surveys. These results were obtained with the UltraVISTA DR1 [73], COSMOS2015 and SPLASH (this work), and FDF [13] catalogs, all considering $H_0 = 70$ km/s/Mpc. There is a clear tendency for decreasing values of D at $z > 1$ in virtually all results, as theoretically predicted (see Sect. 1 above). Such a decrease is, nonetheless, less pronounced in the SPLASH data, which is the only galaxy distribution shown here to have been surveyed in the southern hemisphere

	UVista DR1 $z < 1.0$	$(0.2 < z < 4)$ $z > 1.0$	COSMO2015 $z < 1.0$	$(0.1 < z < 4)$ $z > 1.0$	SPLASH $z < 1.0$	$(0.1 < z < 4)$ $z > 1.0$	FDF $z \lesssim 1.2$	$(0.45 < z < 5)$ $z \gtrsim 1.2$
D_L	1.40 ± 0.02	0.32 ± 0.01	1.22 ± 0.02	0.30 ± 0.01	0.89 ± 0.01	0.48 ± 0.01	1.2 ± 0.3	0.5 ± 0.2
D_z	1.61 ± 0.02	0.38 ± 0.02	1.41 ± 0.01	0.37 ± 0.02	1.01 ± 0.02	0.58 ± 0.02	1.5 ± 0.4	0.6 ± 0.2
D_G	1.75 ± 0.03	0.81 ± 0.06	1.55 ± 0.01	0.76 ± 0.05	1.09 ± 0.03	1.15 ± 0.03	1.8 ± 0.3	1.0 ± 0.7

and $M_{\mathrm{NUV}} - M_{\mathrm{r}} > 3.1$, while the others were considered star-forming.

Regarding the SPLASH survey, following [18,39] we separated the galaxy sample using the *specific star formation rate* (SSFR). Galaxies with $\log \mathrm{SSFR} < -11$ were classified as quiescent, whereas the ones with $\log \mathrm{SSFR} > -11$ were set as star-forming. SSFR is the ratio between star formation rate and stellar mass, being a simple way of quantifying in a uniform way the degree of star formation. Such division by stellar mass gives an indication of how strong is the star formation in a certain galaxy, this being especially important when comparing galaxies having different sizes and masses. In [40] such classification approach was compared to the color–color selection applied to COSMOS2015, and they showed that both methods provide similar results at $z < 1$, but towards high redshift the classification based on the SSFR tends to be more conservative.

Considering the criteria above two subsamples were generated for each survey. Figure 10 shows histograms of redshift distribution of both subsamples up to $z = 4$, where it is clear that the number of blue star forming galaxies is much higher than the red quiescent ones. This selection led the COSMOS2015 survey ending up with 527899 star forming galaxies and 31424 quiescent ones. The SPLASH had respectively 359021 and 20045 galaxies. These four subsamples were then subjected to the same volume-limited filtering process of absolute magnitude cutoff as defined by Eq. (12). Figure 11 shows the outcome of this filtering procedure, which in the end left the COSMOS2015 subsamples further reduced to 208,005 blue galaxies and 22,824 red ones, whereas the filtered SPLASH catalog subsamples respectively ended up with 205,012 and 13,491 galaxies.

The selected and filtered galaxies of the four subsamples had their γ_i^* number densities calculated using the same procedure as described in Sect. 3.4 above. The resulting data points were then linear fitted against their respective distance measures d_i ($i = G, L, z$). Figures 12, 13, 14 and 15 show the decaying power-law curves and actual data fits in the ranges $z < 1$ and $1 \leq z \leq 4$. In view of the results presented in Tables 1, 2, 3 and 4, which showed robustness of the fractal dimension against changes in the Hubble constant, in this Section we calculated all results using only $H_0 = 70$ km/s/Mpc.

The fractal dimensions obtained from the graphs in Figs. 12, 13, 14 and 15 are collected in Table 6, which provides results that can now be compared with the 3rd to 6th columns of Table 5. The blue COSMOS2015 galaxies had their fractal dimensions basically unchanged from the unselected samples, whereas the blue SPLASH ones had D somewhat increased for $z < 1$, but remained basically unchanged for $z > 1$ within the uncertainties. The fractal dimensions of the quiescent galaxies had, nonetheless, the most noticeable changes. For $z < 1$ the red COSMOS2015 had bigger values for D in all distances measures, but suffered a considerable fractal dimension reduction for the $z > 1$. This same considerable decrease in D also happened for the red SPLASH galaxies in both ranges, $z < 1$ and $z > 1$. Finally, the theoretical prediction for the reduction of the fractal dimension in the range $z > 1$ is also observed in all cases and for all distance measures.

6 Conclusions

This paper extended the study of [73] by applying the same fractal analysis methodology to much larger galaxy samples in order to empirically test if large-scale galaxy distributions can be described as fractal systems and if galaxy types, however they are defined or observed, could possibly be dependent on the single fractal dimension D. Tools originally developed for Newtonian hierarchical cosmology were extended and applied to relativistic cosmological models in order to describe possible galaxy fractal structures by means of D at deep redshift scales. These tools were applied to the COSMOS2015 and SPLASH galaxy survey datasets comprising almost one million objects spanning the redshift interval of $0.1 \leq z \leq 6$.

In order to obtain volume-limited subsamples, absolute magnitudes were calculated using the measured redshifts in order to obtain the respective luminosity distances d_L by

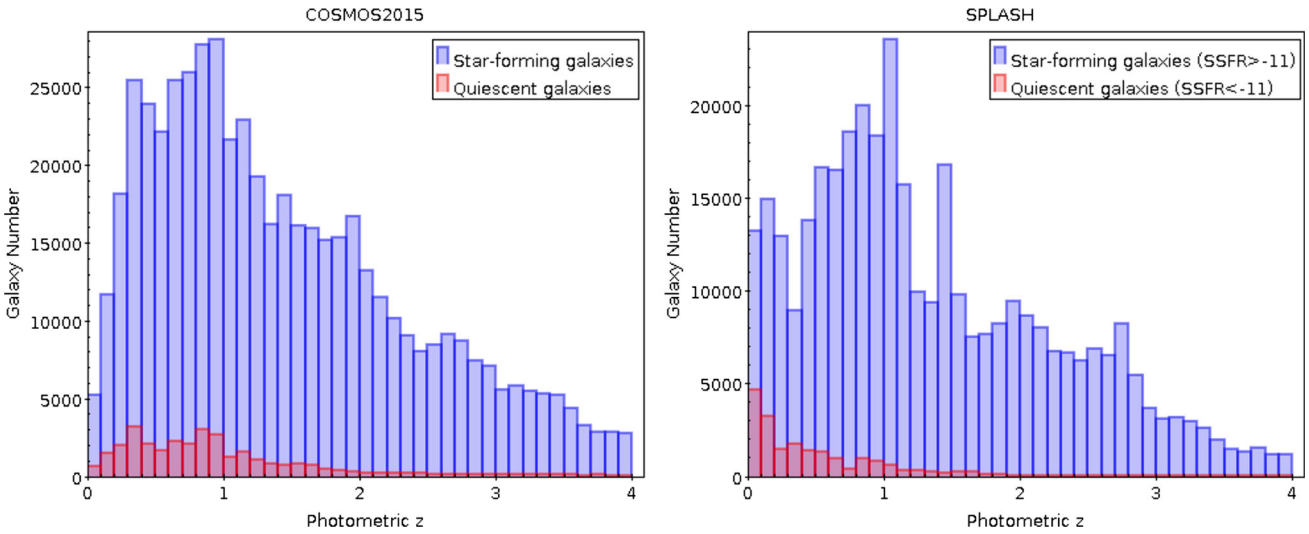

Fig. 10 Histograms showing the galaxy distribution numbers in terms of the redshift for the COSMOS2015 (left) and SPLASH (right) subsamples of blue star forming galaxies and red quiescent ones. Labels are as in the legends. The COSMOS2015 galaxies were separated by color and SPLASH galaxies were classified considering the *specific stellar formation rate* (SSFR) using -11 as the cutoff value (see the main text). Clearly the number of blue galaxies is much higher than the red ones in both surveys

Table 6 Fractal dimensions calculated in the selected blue-star-forming and red-quiescent and then volume-limit-filtered galaxy subsamples of the COSMOS2015 and SPLASH redshift surveys in the range $z \leq 4$. The single fractal dimensions D_L, D_z and D_G were obtained from the galaxy distributions respectively using the luminosity distance d_L, redshift distance d_z and galaxy area distance (transverse comoving distance) d_G. The results were calculated considering only $H_0 = 70$ km/s/Mpc (see the main text). A comparison of these figures with the ones in the 3rd to 6th columns of Table 5 shows that the fractal dimensions do vary according to the blue-red selection used here, this being especially the case for the quiescent galaxies. In addition, as in the results shown in Table 5, all values of D decrease in the range $z > 1$, in some cases quite substantially

	Blue COSMOS2015 $z < 1.0$	$(0.1<z<4)$ $z > 1.0$	Blue SPLASH $z < 1.0$	$(0.1<z<4)$ $z > 1.0$	Red COSMOS2015 $z < 1.0$	$(0.1 < z < 4)$ $z > 1.0$	Red SPLASH $z < 1.0$	$(0.1<z<4)$ $z > 1.0$
D_L	1.21 ± 0.02	0.31 ± 0.01	1.01 ± 0.01	0.51 ± 0.01	1.28 ± 0.02	0.18 ± 0.01	0.49 ± 0.01	0.10 ± 0.01
D_z	1.41 ± 0.01	0.39 ± 0.02	1.15 ± 0.01	0.62 ± 0.02	1.48 ± 0.02	0.22 ± 0.02	0.56 ± 0.01	0.13 ± 0.01
D_G	1.54 ± 0.01	0.80 ± 0.05	1.24 ± 0.03	1.22 ± 0.03	1.61 ± 0.03	0.48 ± 0.05	0.61 ± 0.02	0.26 ± 0.02

assuming the ΛCDM relativistic cosmological model and the apparent magnitude limit of 24.7 in the K-band. Then graphs of absolute magnitudes in the K-band versus redshifts were plotted using three values for the Hubble constant, $H_0 = (65, 70, 75)$ km/s/Mpc. Objects whose absolute magnitudes were above the respective apparent magnitude limit were disregarded, as well as those having $z > 4$. This procedure provided two subsamples with about 402k objects, the first containing 230705 COSMOS2015 galaxies, and the second containing 171548 SPLASH ones. Fractal analysis was then performed in these two subsamples

As relativistic cosmologies have several definitions of observed distance [21], only three distinct ones were used here, namely d_L, the redshift distance d_z and the galaxy area distance d_G, also known as transverse comoving distance. The use of several cosmological distance measures comes from the fact that relativistic effects become strong enough for redshift ranges larger than $z \gtrsim 0.1 - 0.2$ [55], so these distance definitions produce different results for the same redshift value at those ranges. An algorithm for sorting the data was performed so that graphs of number densities vs. relativistic distances were plotted. Straight lines were then fitted to the data in two scales, $z < 1$ and $1 \leq z \leq 4$, whose slopes allowed direct determination of the respective single fractal dimensions.

The results indicated two consecutive redshift ranges behaving as single fractal structures in both catalogs. Rounding them off and their respective uncertainties we found that for $z < 1$ the COSMOS2015 galaxies produced $D = 1.4 \pm 0.2$, whereas the SPLASH galaxies yielded $D = 1.0 \pm 0.1$. For $1 \leq z \leq 4$ the respective calculations produced $D = 0.5 \pm 0.3$ and $D = 0.8 \pm 0.4$. These results were

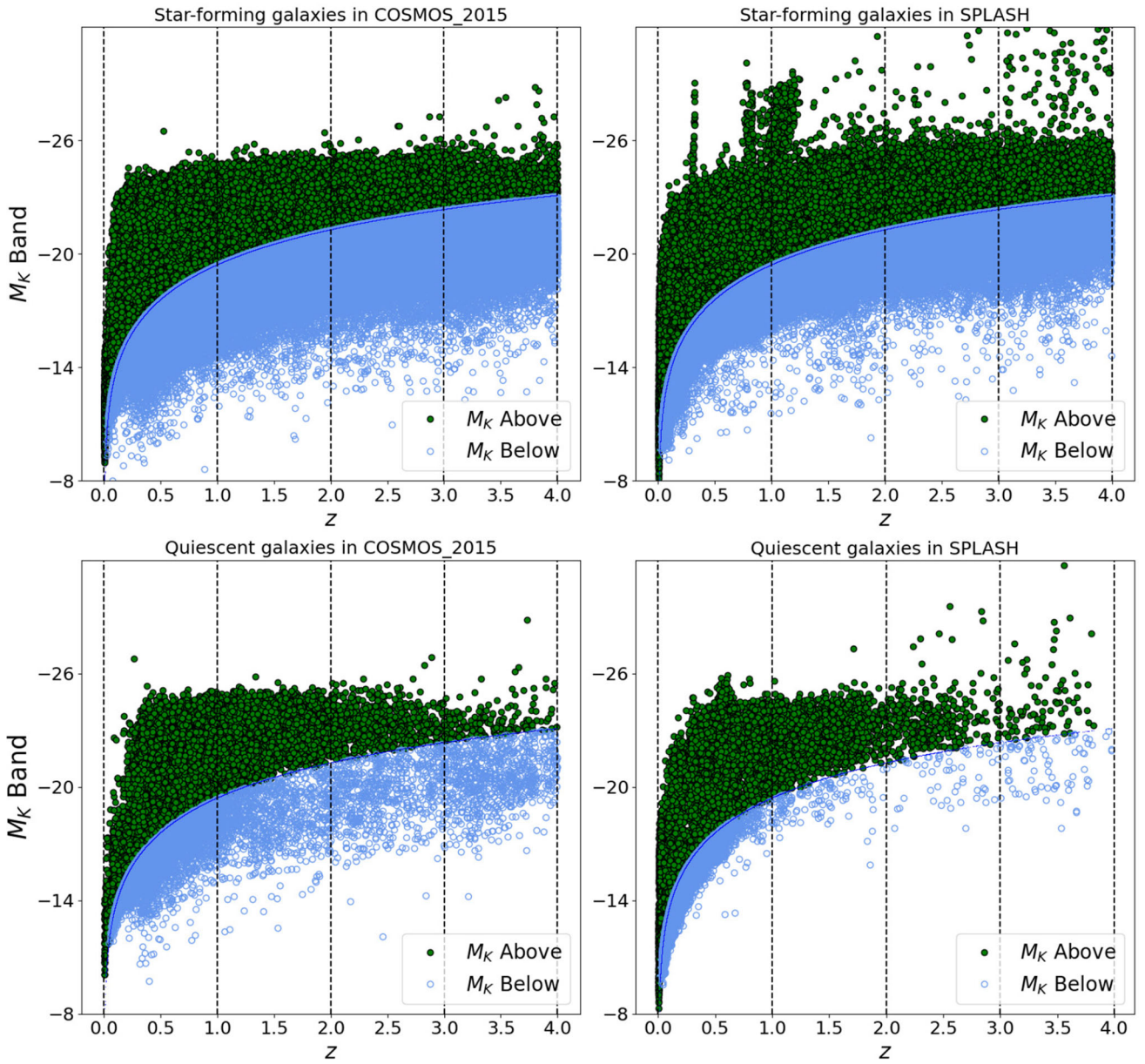

Fig. 11 Plots of the absolute magnitudes for the blue star forming galaxies (top), and red quiescent ones (bottom) for the COSMOS2015 (left) and SPLASH (right) surveys in terms of their photometrically measured redshift values. Specific discriminations are as in the title of each plot. As in Figs. 2 and 3, the dividing line corresponds to apparent magnitude K $= 24.7$, so only blue and red galaxies having M_K above this cutoff and $z \leq 4$ were included in the blue and red COSMOS2015 and SPLASH subsamples. Since previous results indicate that the fractal dimension is not affected by varying the Hubble constant within its currently accepted uncertainty, here only $H_0 = 70$ km/s/Mpc was assumed

found to be unaffected by changes in the Hubble constant within the assumed uncertainty. In addition, no transition to observational homogeneity was found in the data.

Subsamples were created by selecting blue star forming galaxies and red quiescent ones from both the COSMOS2015 and SPLASH surveys. These subsamples were subsequently filtered by the same absolute magnitude limits applied to the unselected samples, resulting in datasets that were used to generate number densities and then to calculate fractal dimensions. The results showed that up to two decimal digits the fractal dimensions of blue galaxies remained basically unchanged, whereas some red galaxies showed noticeable reduction at the same precision, especially the red SPLASH galaxies at both ranges $z < 1$ and $1 \leq z < 4$. This indicates that the fractal dimensions of both surveys are dominated by blue galaxies.

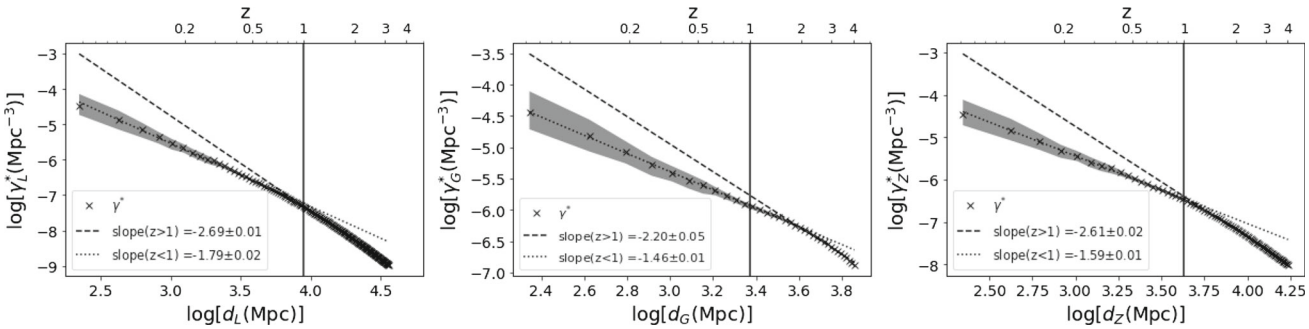

Fig. 12 Log–log graph of γ_L^*, γ_G^* and γ_z^* respectively vs. d_L, d_G and d_z obtained with the blue COSMOS2015 star forming galaxy subsample in the ranges $z < 1$ and $1 \leq z \leq 4$ and respective distance measures. All results were obtained considering $H_0 = 70$ km/s/Mpc

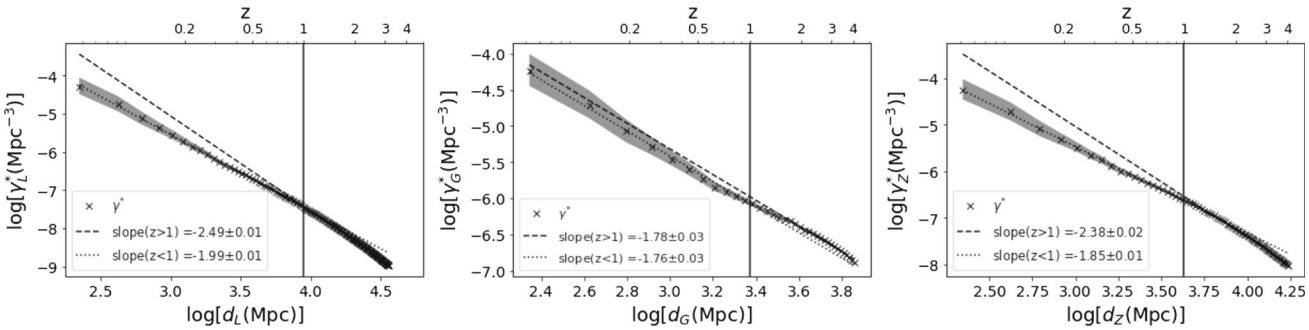

Fig. 13 Log–log graph of γ_L^*, γ_G^* and γ_z^* respectively vs. d_L, d_G and d_z obtained with the blue SPLASH star forming galaxy subsample in the ranges $z < 1$ and $1 \leq z \leq 4$ and respective distance measures. All results were obtained considering $H_0 = 70$ km/s/Mpc

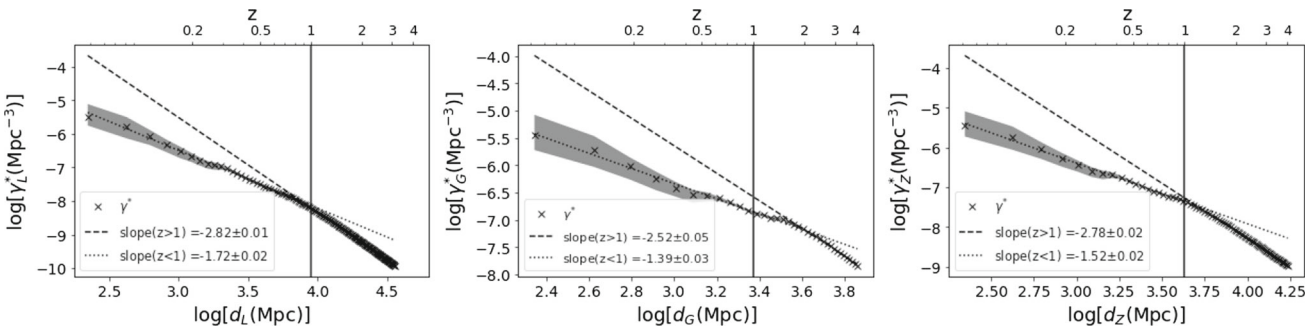

Fig. 14 Log–log graph of γ_L^*, γ_G^* and γ_z^* respectively vs. d_L, d_G and d_z obtained with the red COSMOS2015 quiescent galaxy subsample in the ranges $z < 1$ and $1 \leq z \leq 4$ and respective distance measures. All results were obtained considering $H_0 = 70$ km/s/Mpc

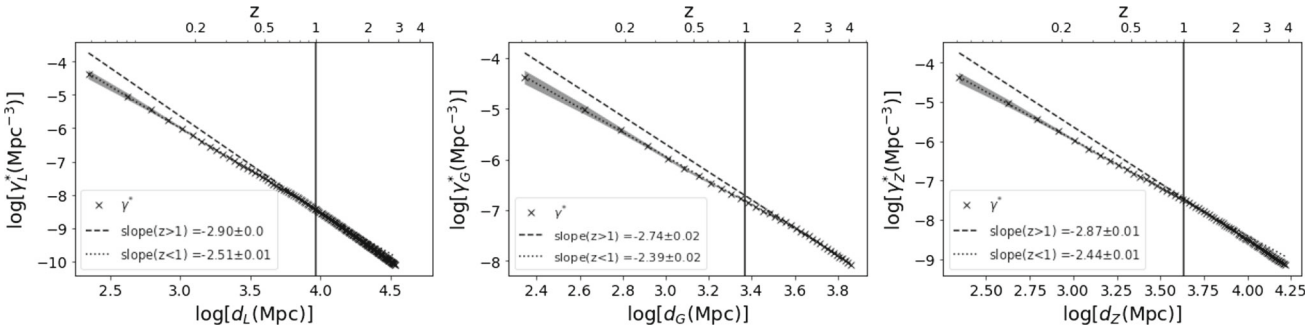

Fig. 15 Log–log graph of γ_L^*, γ_G^* and γ_z^* respectively vs. d_L, d_G and d_z obtained with the red SPLASH quiescent galaxy subsample in the ranges $z < 1$ and $1 \leq z \leq 4$ and respective distance measures. All results were obtained considering $H_0 = 70$ km/s/Mpc

These results suggest that besides being descriptors of galaxy distributions, the fractal dimensions could also be useful tools as tracers of galaxy types and evolution. For this purpose the galaxy number densities could be used directly as depicted here to obtain fractal dimensions or, complementarily, by means of their respective power spectra [45], in order to study distributions consisting of several galactic types, however they are defined or observed, and in different environments.

Therefore, generating subsamples of blue and red galaxies showed not only that the overall theoretical expectations for the fractal dimension remain valid at $z > 1$, but also that the difference between the behaviour of blue versus red galaxies indicate that the fractal dimension can reliably be used as a tool to characterise populations of different types in galaxy formation. So, one could think of further subsample separations in order to study certain types of evolving galaxies or other objects based on their fractal dimension. Under this perspective the fractal dimension would be seen as an intrinsic property of the distribution of objects in the Universe that could be modulated depending on the types of galaxies formed, which means that D can be used as a tool to study different galaxy populations.

It is also important to emphasize that the results reached here are dependent on the way this paper defines homogenity and its possible detection. As noted above the FLRW cosmology is homogeneous by construction in a purely geometrical sense, and as observations go further along the past light cone the spatial homogeneity of the model cannot possibly be observed *in a cumulative manner* at larger scales because the model becomes increasingly observationally inhomogeneous even using almost all distance measures to derive observational density [62]. At small redshifts this effect is not noticeable because the present time hypersurface superposes on the past light cone, but at ranges $z \gtrsim 0.1 - 0.2$ they start to differentiate, rendering this distinction observable in principle [55].

One way of detecting this observational inhomogeneity is by using the set of tools advanced by the pioneers of hierarchical (fractal) cosmology [17,53,74,75] once they are appropriately extended to the relativistic setting, namely, using observational distances, radially observed cumulative number counts and radial densities derived from the latter. The cumulative number counts is connected to the single fractal dimension D which is then used either as tracer of this observational inhomogeneity, or the evolution of galaxy types, or both as have been done in this paper.

The tension mentioned above about a possible transition to homogeneity in the large-scale galaxy distribution can then be attributed to the application of different concepts, tools and methods for dealing with this issue. For instance, Scrimgeour et al. [67] and Gonçalves et al. [30] analyzed their data using the mean number of galaxies in spheres up to a certain comoving distance, the so-called counts-in-sphere, a concept quite different from the radial cumulative number counts $N_{\rm obs}$ used here to define our key quantity $\gamma^*_{\rm obs}$ as shown in Eqs. (2) and (3). Hence, different definitions and methods lead to different results. This should come as no surprise because as it happens with cosmological distances there is no unique way to define homogeneity in cosmology. Each definition and its related methodology produce their own tools which lead to different conclusions about their particularly adopted concept of homogeneity.

Finally, the results presented here raise similar questions as discussed in [73], which are why there is such a significant decrease in the fractal dimension for redshift values larger than unity. This could be an observational effect caused by data bias, due to the simple fact that many galaxies located beyond $z = 1$ are not detected, reducing then the observed galaxy clustering and, therefore, the associated fractal dimension. Other possibility is of some bias associated to the small angular areas of these surveys such that they would not yield representative measurements of the entire sky distribution.

It has been previously thought that different cosmological parameters could affect these results, but this possibility no longer appears plausible since we have used here different values for the Hubble constant in the calculations, and that only altered D very slightly, even so within the obtained uncertainties. This suggests that fractal dimension results are robust to changes in the cosmological model, at least as far as FLRW, or FLRW like, cosmologies are concerned.

Apart from possible observational biases, one might also attribute the decrease in the fractal dimension to real physical effects. Under this viewpoint galaxy evolution and large-scale structure dynamics of the Universe are at play in causing such a decrease. So, it is possible that D changes with the redshift due to galaxy evolution such as selection effects or, perhaps, change in the anisotropy distribution of the underlying cosmology. In this sense the change in D signifies that there might be indeed much less galaxies at high z, meaning that the Universe was void dominated at those epochs because galaxies would be much more sparsely distributed and in reduced numbers. This possibility is not far fetched, since for some time there has been a theoretical prediction stating that the galaxy distribution fractal dimension must indeed fall at larger scales because theory forecasts a sharp decrease in the observed number density at $z > 1$ [57], Fig. 1; [60], Figs. 1 and 3; [62], Fig. 2. Hence, the observational shift in D to smaller values in terms of higher z as reported here and in previous studies could be interpreted as simply the empirical verification of this theoretical prediction.

Acknowledgements We thank a referee for very helpful and useful suggestions which improved this paper. We are also grateful to the editor for useful comments. S.T. thanks the Universidade Federal do Rio de Janeiro for a PIBIC scholarship. A.R.L. is grateful to Brazil's National

Council for Scientific and Technological Development (CNPq) for the financial support.

Data Availability Statement The data underlying this article are available in COSMOS2015 and SPLASH databases, respectively at https://ftp.iap.fr/pub/from_users/hjmcc/COSMOS2015/ and https://www-users.cse.umn.edu/~mehta074/splash/. The datasets were derived from sources in the public domain: https://cosmos.astro.caltech.edu/page/photom and http://splash.caltech.edu/public/catalogs.html.

Declarations

Conflict of interest The authors have no competing interests to declare that are relevant to the content of this article.

Funded by SCOAP[3]. SCOAP[3] supports the goals of the International Year of Basic Sciences for Sustainable Development.

References

1. E. Abdalla, C.B.M.H. Chirenti, Phys. A **337**, 117 (2004)
2. E. Abdalla, N. Afshordi, K. Khodjasteh, R. Mohayaee, A&A **345**, 22 (1999)
3. E. Abdalla, R. Mohayaee, M.B. Ribeiro, Fractals **9**, 451 (2001). https://doi.org/10.1142/S0218348X0100083X
4. V.V.L. Albani, A.S. Iribarrem, M.B. Ribeiro, W.R. Stoeger, ApJ **657**, 760 (2007). https://doi.org/10.1086/510520
5. C.M. Amoroso, Ann. Braz. Acad. Sci. (in Brazilian Portuguese) **51**, 1 (1929)
6. S. Arnouts et al., MNRAS **329**, 355 (2002). https://doi.org/10.1046/j.1365-8711.2002.04988.x
7. S.L. Cacciatori, A. Marrani, F. Re, Int. J. Mod. Phys. D **30**, 2150086 (2021). https://doi.org/10.1142/S0218271821500863
8. E.F. Carpenter, ApJ **88**, 344 (1938). https://doi.org/10.1086/143987
9. C.A. Chacón-Cardona, R. Casas-Miranda, J. Muñoz-Cuartas, Chaos Solitons Fractals **82**, 22 (2016). https://doi.org/10.1016/j.chaos.2015.10.029
10. C.V.L. Charlier, Ark. Mat. Astr. Fys. **4**, 1 (1908)
11. C.V.L. Charlier, Ark. Mat. Astr. Fys. **16**, 1 (1922)
12. P.H. Coleman, L. Pietronero, Phys. Rep. **213**, 311 (1992)
13. G. Conde-Saavedra, A. Iribarrem, M.B. Ribeiro, Phys. A **417**, 332 (2015). https://doi.org/10.1016/j.physa.2014.09.044
14. L. Cosmai, G. Fanizza, F. Sylos Labini, L. Pietronero, L. Tedesco, Class. Quantum Gravity **36**, 045007 (2019). https://doi.org/10.1088/1361-6382/aae8f7
15. G. De Marzo, F. Sylos Labini, L. Pietronero, A&A **651**, A114 (2021). https://doi.org/10.1051/0004-6361/202141081
16. G. de Vaucouleurs, ApJ **131**, 585 (1960)
17. G. de Vaucouleurs, Science **167**, 1203 (1970). https://doi.org/10.1126/science.167.3922.1203
18. H. Domínguez Sánchez et al., MNRAS **417**, 900 (2011). https://doi.org/10.1111/j.1365-2966.2011.19263.x
19. A. Einstein, Ann. Phys. **69**, 436 (1922)
20. Ellis G. F. R., 1971, in Sachs R. K., ed., General Relativity and Cosmology: Proceedings of the International School of Physics "Enrico Fermi", Course 47. Academic Press, New York, pp 104–182. Reprinted in Gen. Rel. Grav., 41 (2009) p. 581–660 https://doi.org/10.1007/s10714-009-0760-7
21. G.F.R. Ellis, Gen. Relativ. Gravit. **39**, 1047 (2007). https://doi.org/10.1007/s10714-006-0355-5
22. I.M.H. Etherington, Philos. Mag. **15**, 761 (1933). https://doi.org/10.1007/s10714-007-0447-x. Reprinted in Gen. Rel. Grav., 39 (2007) 1055
23. A. Gabrielli, L.F. Sylos, M. Joyce, L. Pietronero, *Statistical Physics for Cosmic Structures* (Springer, Berlin, 2005)
24. J. Gaite, Europhys. Lett. (EPL) **71**, 332 (2005). https://doi.org/10.1209/epl/i2005-10082-6
25. J. Gaite, ApJ **658**, 11 (2007). https://doi.org/10.1086/511631
26. J. Gaite, J. Cosmol. Astropart. Phys. **2018**, 010 (2018). https://doi.org/10.1088/1475-7516/2018/07/010
27. J. Gaite, Adv. Astron. **2019**, 6587138 (2019). https://doi.org/10.1155/2019/6587138
28. J. Gaite, Adv. Astron. **2021**, 6680938 (2021). https://doi.org/10.1155/2021/6680938
29. J.E. García-Farieta, R. Casas-Miranda, Chaos Solitons Fractals **111**, 128 (2018). https://doi.org/10.1016/j.chaos.2018.04.018
30. R.S. Gonçalves, G.C. Carvalho, U. Andrade, C.A. Bengaly, J.C. Carvalho, J. Alcaniz, J. Cosmol. Astropart. Phys. **2021**, 029 (2021). https://doi.org/10.1088/1475-7516/2021/03/029
31. M.J. Haggerty, J.R. Wertz, MNRAS **155**, 495 (1972)
32. T. Hockey, V. Trimble, T.R. Williams, K. Bracher, R.A. Jarrell, J.D. Marché, J. Palmeri, D.W.E. Green (eds.), *Biographical Encyclopedia of Astronomers*, 2nd edn. (Springer, New York, 2014). https://doi.org/10.1007/978-1-4419-9917-7
33. R.F.L. Holanda, J.A.S. Lima, M.B. Ribeiro, ApJL **722**, L233 (2010). https://doi.org/10.1088/2041-8205/722/2/L233
34. R.F.L. Holanda, J.A.S. Lima, M.B. Ribeiro, A&A **528**, L14 (2011). https://doi.org/10.1051/0004-6361/201015547
35. R.F.L. Holanda, J.A.S. Lima, M.B. Ribeiro, A&A **538**, A131 (2012). https://doi.org/10.1051/0004-6361/201118343
36. H. Hossienkhani, H. Yousefi, N. Azimi, Int. J. Geom. Methods Mod. Phys. **15**, 1850200 (2018)
37. O. Ilbert et al., A&A **439**, 863 (2005). https://doi.org/10.1051/0004-6361:20041961
38. O. Ilbert et al., A&A **457**, 841 (2006). https://doi.org/10.1051/0004-6361:20065138
39. O. Ilbert et al., ApJ **709**, 644 (2010). https://doi.org/10.1088/0004-637X/709/2/644
40. O. Ilbert et al., A&A **556**, A55 (2013). https://doi.org/10.1051/0004-6361/201321100
41. A.S. Iribarrem, A.R. Lopes, M.B. Ribeiro, W.R. Stoeger, A&A **539**, A112 (2012). https://doi.org/10.1051/0004-6361/201117535
42. A. Jawad, S. Butt, S. Rani, K. Asif, Eur. Phys. J. C **79**, 926 (2019)
43. B.J.T. Jones, V.J. Martínez, E. Saar, J. Einasto, ApJL **332**, L1 (1988). https://doi.org/10.1086/185254
44. C. Laigle et al., ApJS **224**, 24 (2016). https://doi.org/10.3847/0067-0049/224/2/24
45. A.R. Lopes, M.B. Ribeiro, W.R. Stoeger, Eur. Phys. J. Plus **137**, 942 (2022). https://doi.org/10.1140/epjp/s13360-022-03168-7
46. B.B. Mandelbrot, *The Fractal Geometry of Nature* (Freeman, New York, 1983)
47. V.J. Martínez, Vistas Astron. **33**, 337 (1990)

48. V. Mehta et al., ApJS **235**, 36 (2018). https://doi.org/10.3847/1538-4365/aab60c
49. J.R. Mureika, J. Cosmol. Astropart. Phys. **2007**, 021 (2007)
50. J.R. Mureika, C.C. Dyer, Gen. Relativ. Gravit. **36**, 151 (2004)
51. F.A.M.G. Nogueira, Master's thesis, Valongo Observatory, Universidade Federal do Rio de Janeiro (2013). arXiv:1312.5005
52. J. Pan, P. Coles, MNRAS **318**, L51 (2000)
53. L. Pietronero, Phys. A **144**, 257 (1987). https://doi.org/10.1016/0378-4371(87)90191-9
54. V. Raj, M.S. Swapna, S. Soumya, S. Sankararaman, Indian J. Phys. (2019). https://doi.org/10.1007/s12648-019-01400-2
55. L.J. Rangel Lemos, M.B. Ribeiro, A&A **488**, 55 (2008). https://doi.org/10.1051/0004-6361:20077978
56. M.B. Ribeiro, ApJ **388**, 1 (1992). https://doi.org/10.1086/171123
57. M.B. Ribeiro, ApJ **395**, 29 (1992). https://doi.org/10.1086/175374
58. M.B. Ribeiro, ApJ **415**, 469 (1993). https://doi.org/10.1086/175374
59. M.B. Ribeiro, in *Deterministic Chaos in General Relativity* ed. by D.W. Hobill, A. Burd, A. Coley, vol. 332. (Plenum, New York, 1994), p. 269. https://doi.org/10.1007/978-1-4757-9993-4_15. arXiv:0910.4877
60. M.B. Ribeiro, ApJ **441**, 477 (1995). https://doi.org/10.1086/175374
61. M.B. Ribeiro, Fractals **9**, 237 (2001). https://doi.org/10.1142/S0218348X01000646
62. M.B. Ribeiro, Gen. Relativ. Gravit. **33**, 1699 (2001). https://doi.org/10.1023/A:1013095316494
63. M.B. Ribeiro, A&A **429**, 65 (2005). https://doi.org/10.1051/0004-6361:20041469
64. M.B. Ribeiro, A.Y. Miguelote, Braz. J. Phys. **28**, 132 (1998). https://doi.org/10.1590/S0103-97331998000200007
65. E. Sadri, M. Khurshudyan, S. Chattopadhyay, Astrophys. Space Sci. **363**, 230 (2018)
66. N. Scoville et al., Astrophys J. Suppl. Ser. **172**, 1 (2007). https://doi.org/10.1086/516585
67. M.I. Scrimgeour et al., MNRAS **425**, 116 (2012). https://doi.org/10.1111/j.1365-2966.2012.21402.x
68. F. Selety, Ann. Phys. **68**, 281 (1922)
69. B.J. Souza, Master's thesis, Physics Institute, Universidade Federal do Rio de Janeiro (2020): in Brazilian Portuguese. https://www.if.ufrj.br/~mbr/students-M.B.Ribeiro/dissertacao-Bruno.pdf
70. C. Stahl, Int. J. Mod. Phys. D **25**, 1650066 (2016)
71. L.F. Sylos, Class. Quantum Gravity **28**, 164003 (2011)
72. L.F. Sylos, M. Montuori, L. Pietronero, Phys. Rep. **293**, 61 (1998)
73. S. Teles, A.R. Lopes, M.B. Ribeiro, Phys. Lett. B **813**, 136034 (2021). https://doi.org/10.1016/j.physletb.2020.136034
74. J.R. Wertz, (1970), PhD thesis, University of Texas at Austin
75. J.R. Wertz, ApJ **164**, 227 (1971). https://doi.org/10.1086/150834
76. P.S. Wesson, Astrophys. Space Sci. **54**, 489 (1978). https://doi.org/10.1007/BF00639451
77. R.J. Williams, R.F. Quadri, M. Franx, P. van Dokkum, I. Labbé, ApJ **691**, 1879 (2009). https://doi.org/10.1088/0004-637X/691/2/1879